

Inspiration from Intersecting D-branes: General Supersymmetry Breaking Soft Terms in No-Scale \mathcal{F} - $SU(5)$

Ron De Benedetti,¹ Chuang Li,^{2,3} Tianjun Li,^{2,3} Adam Lux,⁴ James A. Maxin,¹ and Dimitri V. Nanopoulos^{5,6,7}

¹*Department of Chemistry and Physics, Louisiana State University, Shreveport, Louisiana 71115 USA*

²*CAS Key Laboratory of Theoretical Physics, Institute of Theoretical Physics,
Chinese Academy of Sciences, Beijing 100190, China*

³*School of Physical Sciences, University of Chinese Academy of Sciences, No.19A Yuquan Road, Beijing 100049, China*

⁴*Department of Physics and Engineering Physics,
The University of Tulsa, Tulsa, OK 74104 USA*

⁵*George P. and Cynthia W. Mitchell Institute for Fundamental Physics and Astronomy,
Texas A&M University, College Station, TX 77843, USA*

⁶*Astroparticle Physics Group, Houston Advanced Research Center (HARC), Mitchell Campus, Woodlands, TX 77381, USA*

⁷*Academy of Athens, Division of Natural Sciences,
28 Panepistimiou Avenue, Athens 10679, Greece*

Motivated by D-brane model building, we evaluate the \mathcal{F} - $SU(5)$ model with additional vector-like particle multiplets, referred to as flippons, within the framework of No-Scale Supergravity with non-vanishing general supersymmetry breaking soft terms at the string scale. The viable phenomenology is uncovered by applying all current experimental constraints, including but not limited to the correct light Higgs boson mass, WMAP and Planck relic density measurements, and several LHC constraints on supersymmetric particle spectra. Four interesting regions of the parameter space arise, as well as mixed scenarios, given by: (i) light stop coannihilation; (ii) pure Higgsino dark matter; (iii) Higgs funnel; and (iv) light stau coannihilation. All regions can generate the observed value of the relic density commensurate with a 125 GeV light Higgs boson mass, with the exception of the relatively small relic density value for the pure Higgsino lightest supersymmetric particle (LSP). This work is concluded by gauging the model against present LHC search constraints and derivation of the final states observable at the LHC for each of these scenarios.

PACS numbers: 11.10.Kk, 11.25.Mj, 11.25.-w, 12.60.Jv

INTRODUCTION

Successful confirmation of the Standard Model (SM) was celebrated when the lightest CP-even Higgs boson with mass $m_h = 125.09 \pm 0.24$ GeV was discovered at the LHC in 2012 [1, 2]. Despite the memorable occasion, severe anomalies persisted in the SM, for instance, the gauge hierarchy problem, conspicuous absence of gauge coupling unification, and lack of a plausible dark matter candidate, just to highlight a few. Beyond the SM (BSM) theories, and supersymmetry in particular, can rescue high-energy physics from these SM deficiencies. Supersymmetry (SUSY) can solve the gauge hierarchy problem and produce gauge coupling unification. In supersymmetric SMs (SSMs), the large top quark Yukawa coupling can radiatively break electroweak (EW) gauge symmetry. The lightest supersymmetric particle (LSP) neutralino ($\tilde{\chi}_1^0$) can serve as a viable dark matter candidate in SSMs with R -parity. Of particular significance, gauge coupling unification strongly suggests Grand Unified Theories (GUTs), and SUSY GUTs can be elegantly constructed from superstring theory. Supersymmetry thus provides rather auspicious new physics beyond the SM, beautifully merging low energy phenomenology with high-energy fundamental physics. Despite the successful intervention SUSY can inject into high-energy physics, it remains considerably challenging

to obtain a light Higgs boson mass around 125 GeV in the Minimal SSM (MSSM) without embracing either multi-TeV top squarks with small mixing or TeV-scale top squarks with large mixing [3]. Compounding the effort are the strong constraints on the SSM viable parameter space established by the LHC SUSY searches. Principally among those LHC constraints are the masses for the gluino (\tilde{g}) and light stop (\tilde{t}_1), where the nominal exclusion curves imply the masses are heavier than about 1.9 TeV and 900 GeV, respectively [4], indicating that an electroweak fine-tuning problem may potentially lurk in SUSY.

The aforementioned threats to developing effective BSM constructions notwithstanding, string theory perseveres as one of the most promising theories for quantum gravity. As opposed to the conventional unification at the GUT scale realized in the typical SUSY GUT, we proposed the testable flipped $SU(5) \times U(1)_X$ models [5–7] with additional TeV-scale vector-like particles [8], which we colorfully dubbed flippons, to obtain gauge coupling unification at the *string scale*. Subsequently, we further constructed this class of flipped $SU(5)$ models from local F-theory model building [9, 10]. These flipped $SU(5)$ models with extra vector-like multiplets can be realized in free-fermionic string constructions also [11], hence we denoted them \mathcal{F} - $SU(5)$. Let's enumerate the “Miracles” [12] of the flippons in \mathcal{F} - $SU(5)$:

(1) The lightest CP-even Higgs boson mass can be easily lifted to 125 GeV due to one-loop contributions from the Yukawa couplings between the flippons and Higgs fields [12, 13].

(2) It is well-known that dimension-five proton decays mediated by colored Higgsinos are highly suppressed due to the missing partner mechanism and TeV-scale μ term in the flipped $SU(5) \times U(1)_X$ models. In \mathcal{F} - $SU(5)$, the $SU(3)_C \times SU(2)_L$ gauge couplings do in fact unify at the traditional GUT scale while the two unified gauge couplings increase as a result of the vector-like particle contributions [14, 15]. Therefore, dimension-six proton decays via heavy gauge boson exchanges are within the reach of the future proton decay experiments such as the Hyper-Kamiokande experiment. More concisely, \mathcal{F} - $SU(5)$ models differ from the minimal flipped $SU(5) \times U(1)_X$ model since the proton lifetime in the minimal model is too lengthy for future proton decay experiments.

(3) The lightest neutralino serves as the LSP and is lighter than the light stau attributable to the longer running of the Renormalization Group Equations (RGEs) in No-Scale supergravity [16], allowing the LSP neutralino to prevail as a dark matter candidate [17–19]. More acutely, No-Scale \mathcal{F} - $SU(5)$ yields the uncommon mass hierarchy $M(\tilde{t}_1) < M(\tilde{g}) < M(\tilde{q})$ of a light stop and gluino both substantially lighter than all other squarks (\tilde{q}) [17–19]. The net effect of this rare SUSY spectrum is the production of four top quarks, leading to large multijet events at the LHC [20].

(4) An alliance between No-Scale supergravity and the Giudice-Masiero (GM) mechanism [21] allows the SUSY electroweak fine-tuning problem to be resolved naturally [22, 23].

Several prior No-Scale \mathcal{F} - $SU(5)$ analyses have intimately examined vanishing SUSY breaking soft terms with the exception of a single unified gaugino parameter $M_{1/2}$ (see, for example, Refs. [12, 24, 25]). To complement those prior sweeping studies, we now consider in this paper non-zero general SUSY breaking soft terms in No-Scale \mathcal{F} - $SU(5)$, partially inspired by D-brane model building [26]. The low-energy particle spectra will be examined that are consistent with all the current experimental constraints, and interesting diverse regions of the parameter space that can generate the observed dark matter relic density and correct light Higgs boson mass, in addition to several other currently operating experiments, will be identified and analyzed discretely to derive low-energy phenomenology. Finally, benchmarks models will be classified and branching fractions computed to itemize the final states observable at the LHC.

THE \mathcal{F} - $SU(5)$ MODEL

Here we only briefly review the minimal flipped $SU(5)$ model [5–7], where the gauge group $SU(5) \times U(1)_X$ can be embedded into the $SO(10)$ model. More comprehensive discussions of the minimal flipped $SU(5)$ model can be found in Refs. [12, 20, 23, 24, 27] and references therein. We define the generator $U(1)_{Y'}$ in $SU(5)$ as

$$T_{U(1)_{Y'}} = \text{diag} \left(-\frac{1}{3}, -\frac{1}{3}, -\frac{1}{3}, \frac{1}{2}, \frac{1}{2} \right), \quad (1)$$

and subsequently the hypercharge is given by

$$Q_Y = \frac{1}{5} (Q_X - Q_{Y'}). \quad (2)$$

We have three families of the SM fermions whose quantum numbers under $SU(5) \times U(1)_X$ are respectively

$$F_i = (\mathbf{10}, \mathbf{1}), \quad \bar{f}_i = (\bar{\mathbf{5}}, -\mathbf{3}), \quad \bar{l}_i = (\mathbf{1}, \mathbf{5}), \quad (3)$$

where $i = 1, 2, 3$. The SM particle assignments in F_i , \bar{f}_i and \bar{l}_i are

$$F_i = (Q_i, D_i^c, N_i^c), \quad \bar{f}_i = (U_i^c, L_i), \quad \bar{l}_i = E_i^c, \quad (4)$$

where Q_i , U_i^c , D_i^c , L_i , E_i^c and N_i^c are the left-handed quark doublets, right-handed up-type quarks, down-type quarks, left-handed lepton doublets, right-handed charged leptons, and neutrinos, respectively. Generation of the heavy right-handed neutrino masses is accomplished by introduction of three SM singlets ϕ_i .

Breaking the GUT and electroweak gauge symmetries is achieved via introduction of the two pairs of Higgs representations

$$\begin{aligned} H &= (\mathbf{10}, \mathbf{1}), \quad \bar{H} = (\bar{\mathbf{10}}, -\mathbf{1}), \\ h &= (\mathbf{5}, -\mathbf{2}), \quad \bar{h} = (\bar{\mathbf{5}}, \mathbf{2}). \end{aligned} \quad (5)$$

The states in the H multiplet are labeled by the same symbols as in the F multiplet, and for \bar{H} we merely add “bar” above the fields. Explicitly, the Higgs particles are

$$H = (Q_H, D_H^c, N_H^c), \quad \bar{H} = (\bar{Q}_{\bar{H}}, \bar{D}_{\bar{H}}^c, \bar{N}_{\bar{H}}^c), \quad (6)$$

$$h = (D_h, D_h, D_h, H_d), \quad \bar{h} = (\bar{D}_{\bar{h}}, \bar{D}_{\bar{h}}, \bar{D}_{\bar{h}}, H_u), \quad (7)$$

where H_d and H_u are one pair of Higgs doublets in the MSSM.

The $SU(5) \times U(1)_X$ gauge symmetry is broken down to the SM gauge symmetry by the following Higgs superpotential at the GUT scale

$$W_{\text{GUT}} = \lambda_1 H H h + \lambda_2 \bar{H} \bar{H} \bar{h} + \Phi (\bar{H} H - M_H^2). \quad (8)$$

Only one F-flat and D-flat direction exists, which can be rotated along the N_H^c and $\bar{N}_{\bar{H}}^c$ directions. Hence, we

obtain $\langle N_H^c \rangle = \langle \overline{N}_{\overline{H}}^c \rangle = M_H$. Furthermore, the superfields H and \overline{H} are “eaten” and acquire substantial masses via the supersymmetric Higgs mechanism, with the exception of D_H^c and $\overline{D}_{\overline{H}}^c$. Additionally, the superpotential terms $\lambda_1 H H h$ and $\lambda_2 \overline{H} \overline{H} \overline{h}$ couple D_H^c and $\overline{D}_{\overline{H}}^c$ respectively with D_h and $\overline{D}_{\overline{h}}$, forming massive eigenstates with masses $2\lambda_1 \langle N_H^c \rangle$ and $2\lambda_2 \langle \overline{N}_{\overline{H}}^c \rangle$. As a result, we naturally experience the doublet-triplet splitting due to the missing partner mechanism [7]. The triplets in h and \overline{h} though only have a small mixing through the μ term, and as such, the colored Higgsino-exchange mediated proton decay is negligible, *i.e.*, there is no dimension-5 proton decay problem.

To realize string-scale gauge coupling unification [8–10], we introduce the following vector-like particles (flippons) at the TeV scale

$$\begin{aligned} XF &= (\mathbf{10}, \mathbf{1}) , \quad \overline{XF} = (\overline{\mathbf{10}}, -\mathbf{1}) , \\ Xl &= (\mathbf{1}, -\mathbf{5}) , \quad \overline{Xl} = (\mathbf{1}, \mathbf{5}) . \end{aligned} \quad (9)$$

The particle content from the decompositions of XF , \overline{XF} , Xl , and \overline{Xl} under the SM gauge symmetry are

$$\begin{aligned} XF &= (XQ, XD^c, XN^c) , \quad \overline{XF} = (XQ^c, XD, XN) , \\ Xl &= XE , \quad \overline{Xl} = XE^c . \end{aligned} \quad (10)$$

The quantum numbers for the extra vector-like particles under the $SU(3)_C \times SU(2)_L \times U(1)_Y$ gauge symmetry are

$$XQ = (\mathbf{3}, \mathbf{2}, \frac{1}{6}) , \quad XQ^c = (\overline{\mathbf{3}}, \mathbf{2}, -\frac{1}{6}) , \quad (11)$$

$$XD = (\mathbf{3}, \mathbf{1}, -\frac{1}{3}) , \quad XD^c = (\overline{\mathbf{3}}, \mathbf{1}, \frac{1}{3}) , \quad (12)$$

$$XN = (\mathbf{1}, \mathbf{1}, \mathbf{0}) , \quad XN^c = (\mathbf{1}, \mathbf{1}, \mathbf{0}) , \quad (13)$$

$$XE = (\mathbf{1}, \mathbf{1}, -\mathbf{1}) , \quad XE^c = (\mathbf{1}, \mathbf{1}, \mathbf{1}) . \quad (14)$$

The superpotential is

$$\begin{aligned} W_{\text{Yukawa}} &= y_{ij}^D F_i F_j h + y_{ij}^{U\nu} F_i \overline{f}_j \overline{h} + y_{ij}^{E\overline{l}} \overline{f}_i \overline{f}_j h \\ &\quad + \mu h \overline{h} + y_{ij}^N \phi_i \overline{H} F_j + M_{ij}^\phi \phi_i \phi_j \\ &\quad + y_{XF} X F X F h + y_{\overline{XF}} \overline{X} \overline{F} \overline{X} \overline{F} \overline{h} \\ &\quad + M_{XF} \overline{X} \overline{F} X F + M_{Xl} \overline{X} \overline{l} X l , \end{aligned} \quad (15)$$

and after the $SU(5) \times U(1)_X$ gauge symmetry is broken down to the SM gauge symmetry, the above superpotential gives

$$\begin{aligned} W_{SSM} &= y_{ij}^D D_i^c Q_j H_d + y_{ji}^{U\nu} U_i^\nu Q_j H_u + y_{ij}^E E_i^c L_j H_d \\ &\quad + y_{ij}^{U\nu} N_i^\nu L_j H_u + \mu H_d H_u + y_{ij}^N \langle \overline{N}_{\overline{H}}^c \rangle \phi_i N_j^c \\ &\quad + y_{XF} X Q X D^c H_d + y_{\overline{XF}} \overline{X} Q^c X D H_u \\ &\quad + M_{XF} (X Q^c X Q + X D^c X D) \\ &\quad + M_{Xl} X E^c X E + M_{ij}^\phi \phi_i \phi_j \\ &\quad + \dots (\text{decoupled below } M_{GUT}). \end{aligned} \quad (16)$$

where y_{ij}^D , $y_{ij}^{U\nu}$, y_{ij}^E , y_{ij}^N , y_{XF} , and $y_{\overline{XF}}$ are Yukawa couplings, μ is the bilinear Higgs mass term, and M_{ij}^ϕ , M_{XF} and M_{Xl} are masses for new particles. These new particles are of course our flippons, however, we shall not explicitly compute the masses M_{ij}^ϕ , M_{XF} , and M_{Xl} here in this work, reserving that project for a future date. Nonetheless, we do implement a common mass decoupling scale M_V for the flippon vector-like particles. Current LHC constraints on vector-like T and B quarks [28] provide lower limits of around 855 GeV for our (XQ, XQ^c) vector-like flippons and 735 GeV for our (XD, XD^c) vector-like flippons. Accordingly, we establish our lower M_V limit at $M_V \geq 855$ GeV to ensure complete coverage of all experimentally viable flippon masses in our analysis.

As summarized in the prior section, the split-unification of flipped $SU(5)$ [5–7] provides for fundamental GUT scale Higgs representations (not adjoints), natural doublet-triplet splitting, suppression of dimension-five proton decay [29], and a two-step see-saw mechanism for neutrino masses [30, 31]. Additions to the one-loop gauge β -function coefficients b_i to include contributions from the vector-like flippon multiplets induce the necessary flattening of the $SU(3)$ Renormalization Group Equation (RGE) running ($b_3 = 0$) [17], translating into a clear separation between the primary $SU(3)_C \times SU(2)_L$ unification near 10^{16} GeV and the secondary $SU(5) \times U(1)_X$ unification at around 5×10^{17} GeV, which we define as the $M_{\mathcal{F}}$ scale, thus elevating unification to near the Planck mass. At the primary $SU(3)_C \times SU(2)_L$ unification near 10^{16} GeV, the M_2 and M_3 gaugino mass terms are unified into a single term that we refer to as M_5 [32], where $M_5 = M_2 = M_3$ between the primary unification around 10^{16} GeV and the secondary $SU(5) \times U(1)_X$ unification near 5×10^{17} GeV [17]. The M_1 gaugino mass term runs up to the secondary $SU(5) \times U(1)_X$ unification at $M_{\mathcal{F}}$ and unifies with M_5 , by means of a slight shift due to $U(1)_X$ flux effects [32] between the primary unification around 10^{16} GeV and the secondary $SU(5) \times U(1)_X$ unification at $M_{\mathcal{F}}$ [17]. Given this shift, we refer to the M_1 gaugino mass term above the primary unification around 10^{16} GeV as M_{1X} [32]. The resulting baseline extension for logarithmic running of the No-Scale boundary conditions permits sufficient scale for natural dynamic evolution down to viable phenomenology at the electroweak scale. It is this associated flattening of the color-charged gaugino mass scale that produces the distinctive mass texture of $M(\tilde{t}_1) < M(\tilde{g}) < M(\tilde{q})$, generating a light stop and gluino that are lighter than all other squarks [12].

Therefore, the most general supersymmetry breaking soft terms at the scale $M_{\mathcal{F}}$ in our \mathcal{F} - $SU(5)$ model are M_5 , M_{1X} , $M_{U^c L}$, M_{E^c} , $M_{Q D^c N^c}$, M_{H_u} , M_{H_d} , A_τ , A_t , and A_b . General supersymmetry breaking soft terms of these type are partially inspired by D-brane model building [26], where F_i , \overline{f}_i , \overline{l}_i , and h/\overline{h} arise from intersections

TABLE I: The \mathcal{F} - $SU(5)$ general SUSY breaking soft terms, in addition to the vector-like flippon decoupling scale M_V , the low energy ratio of Higgs vacuum expectation values (VEVs) $\tan\beta$, and top quark mass M_t , for the four regions of the model space we study in this work. Each benchmark point is identified with an alphabetical label in order to link the data in TABLE I with the data in TABLES II - III. All masses are in GeV.

Model	benchmark	M_5	M_{1X}	$M_{U^c L}$	M_{E^c}	$M_{Q D^c N^c}$	M_H	A_τ	A_t	A_b	M_V	$\tan\beta$	M_t
Stop Coannihilation	A	1650	3125	2142	1158	3125	175	3125	-4850	1250	16250	17.58	174.43
Stop Coannihilation	B	1800	3275	325	3275	3275	1308	325	-4550	-1500	16550	42.74	171.85
Stop Coannihilation	C	2325	3800	850	2817	2325	3800	2600	-3500	2600	17600	24.33	174.56
Pure Higgsino	D	1700	4650	3667	3667	1700	2683	1250	4300	-1800	4055	32.83	173.43
Pure Higgsino	E	2050	5000	3525	5000	5000	5000	-1100	1950	-1100	4755	48.16	174.80
Pure Higgsino	F	2375	3850	2867	3850	2375	3850	-350	2700	-350	2455	36.66	173.26
Higgs Funnel	G	1500	2975	4450	2483	2975	2483	550	3600	-2500	3655	30.83	173.38
Higgs Funnel	H	1750	3225	3225	2242	275	1258	275	1450	-1600	16450	30.41	173.14
Higgs Funnel	I	2300	3775	3775	2792	825	2792	3775	2550	-500	9928	35.91	173.25
Stau Coannihilation	J	1600	1600	125	1108	1600	1108	125	-1900	1150	16150	28.91	173.11
Stau Coannihilation	K	2175	3650	700	1683	700	2667	-750	2300	2300	9678	46.49	171.92
Stau Coannihilation	L	2625	4100	1150	3117	2625	1150	-2900	-2900	3200	2955	50.99	172.01

TABLE II: Relevant SUSY spectrum masses for the \mathcal{F} - $SU(5)$ general SUSY breaking soft terms of TABLE I. The soft SUSY breaking terms that generate each of these spectra can be identified by the alphabetical label. A \dagger symbol in the light Higgs boson mass m_h column represents the theoretically computed value consisting of *only* the 1-loop and 2-loop SUSY contributions, primarily from the coupling to the light stop, but does *not* include any vector-like flippon contributions, whereas a $\dagger\dagger$ symbol represents the 1-loop and 2-loop SUSY contributions *plus* the maximum vector-like flippon contribution. All masses are in GeV.

Model	Benchmark	$M(\tilde{\chi}_1^0)$	$M(\tilde{\chi}_2^0)$	$M(\tilde{\chi}_1^\pm)$	$M(\tilde{\tau}_1^\pm)$	$M(\tilde{t}_1)$	$M(\tilde{u}_R)$	$M(\tilde{g})$	m_h	$M(H^0/A^0)$
Stop Coannihilation	A	693	781	781	1080	729	3759	2225	127.34 †	4484
Stop Coannihilation	B	728	850	850	2058	766	3727	2397	125.85 †	3927
Stop Coannihilation	C	862	1105	1105	2418	895	4370	3020	127.60 †	5134
Pure Higgsino	D	188	-198	192	3729	3012	4695	2246	126.73 ††	1268
Pure Higgsino	E	411	-421	415	3241	3586	5591	2726	126.21 †	1794
Pure Higgsino	F	374	-383	378	3482	3699	5293	3068	125.99 †	2811
Higgs Funnel	G	621	679	679	3326	3556	4909	2028	127.18 ††	1316
Higgs Funnel	H	717	824	824	3045	2729	4172	2337	124.87 ††	1449
Higgs Funnel	I	840	1068	1068	3435	3564	5239	2989	124.67 †	1739
Stau Coannihilation	J	362	749	749	365	1248	2937	2121	126.77 †	3110
Stau Coannihilation	K	799	918	912	802	2729	3985	2805	125.62 ††	1781
Stau Coannihilation	L	870	1177	1177	876	2632	5148	3278	126.43 †	4179

TABLE III: Relic density (Ωh^2), rare decay processes (Δa_μ , $Br(b \rightarrow s\gamma)$, $Br(B_s^0 \rightarrow \mu^+\mu^-)$), rescaled dark matter direct-detection cross sections (σ_{SI} , σ_{SD}), and $p \rightarrow e^+\pi^0$ proton decay rates (τ_p) for the \mathcal{F} - $SU(5)$ general SUSY breaking soft terms of TABLE I. The soft SUSY breaking terms that generate each of these values can be identified by the alphabetical label. The σ_{SI} and σ_{SD} cross-sections have been rescaled in accordance with Eq. (17). The numerical values given for Δa_μ are $\times 10^{-10}$, $Br(b \rightarrow s\gamma)$ are $\times 10^{-4}$, $Br(B_s^0 \rightarrow \mu^+\mu^-)$ are $\times 10^{-9}$, rescaled spin-independent cross-sections σ_{SI} are $\times 10^{-11}$ pb, rescaled spin-dependent cross-sections σ_{SD} are $\times 10^{-9}$ pb, and proton decay rate τ_p are $\times 10^{35}$ yrs.

Model	Benchmark	Ωh^2	Δa_μ	$Br(b \rightarrow s\gamma)$	$Br(B_s^0 \rightarrow \mu^+\mu^-)$	σ_{SI}	σ_{SD}	τ_p	LSP
Stop Coannihilation	A	0.1115	0.40	3.56	3.16	0.1	0.1	3.9	> 99% Bino
Stop Coannihilation	B	0.1219	1.02	3.45	3.57	0.1	0.1	5.9	> 99% Bino
Stop Coannihilation	C	0.1045	0.60	3.47	3.20	0.6	1.0	2.7	> 99% Bino
Pure Higgsino	D	0.0052	0.74	3.72	2.90	34	1471	0.3	> 99% Higgsino
Pure Higgsino	E	0.0198	0.99	3.64	3.08	125	1484	0.8	> 98% Higgsino
Pure Higgsino	F	0.0170	0.93	3.57	3.04	77	1305	0.4	> 98% Higgsino
Higgs Funnel	G	0.1194	0.57	3.71	3.10	15	40.8	2.0	> 99% Bino
Higgs Funnel	H	0.1193	0.76	3.61	3.38	6.4	13.2	2.6	> 99% Bino
Higgs Funnel	I	0.1210	0.77	3.60	3.27	46	112	1.8	> 99% Bino
Stau Coannihilation	J	0.1189	1.81	3.44	3.26	0.3	1.1	2.9	> 99% Bino
Stau Coannihilation	K	0.1202	2.51	3.47	3.54	940	2746	1.3	> 93% Bino
Stau Coannihilation	L	0.1176	0.79	3.49	3.65	0.1	0.1	4.4	> 99% Bino

of different stacks of D-branes. Consequently, the corresponding supersymmetry breaking soft mass terms and trilinear A terms will be different, while M_{H_u} is equal to M_{H_d} . Even though the Yukawa terms HHh and $\bar{H}\bar{H}h$ of Eq. (8) and $F_i F_j h$, $X F X F h$, and $\bar{X} \bar{F} \bar{X} \bar{F} h$ of Eq. (15) are forbidden by the anomalous global $U(1)$ symmetry of $U(5)$, we might generate these Yukawa terms from high-dimensional operators or instanton effects. Unlike the $SU(5)$ models, the Yukawa term $F_i F_j h$ in the \mathcal{F} - $SU(5)$ model gives down-type quark masses, so their Yukawa couplings can be small and can be generated via high-dimensional operators or instanton effects.

NUMERICAL METHODOLOGY

The general SUSY breaking soft terms M_5 , M_{1X} , $M_{U^c L}$, M_{E^c} , $M_{Q D^c N^c}$, $M_{H_u} = M_{H_d} = M_H$, A_τ , A_t , and A_b are applied at the $M_{\mathcal{F}}$ scale near $M_{\mathcal{F}} \simeq 5 \times 10^{17}$ GeV (in contrast to the traditional GUT scale of about 10^{16} GeV in the MSSM), in addition to $\tan\beta$, the vector-like flippon mass decoupling scale M_V , and the top quark mass M_t . The parameter space is sampled within the limits $100 \leq M_5 \leq 5000$ GeV, $100 \leq M_{1X} \leq 5000$ GeV, $100 \leq M_{U^c L} \leq 5000$ GeV, $100 \leq M_{E^c} \leq 5000$ GeV, $100 \leq M_{Q D^c N^c} \leq 5000$ GeV, $-5000 \leq A_\tau \leq 5000$ GeV, $-5000 \leq A_t \leq 5000$ GeV, $-5000 \leq A_b \leq 5000$ GeV, $2 \leq \tan\beta \leq 60$, and $855 \leq M_V \leq 20,000$ GeV. A reasonable tolerance of the top quark mass is permitted around the world average [33], employing upper and lower limits of $171.8 \leq M_t \leq 174.8$ GeV. The WMAP 9-year [34] and 2015 Planck [35] relic density measurements are implemented, such that we constrain the model to satisfy both sets of data and allow the inclusion of multi-component dark matter beyond the neutralino, imposing limits of $\Omega h^2 \leq 0.1221$. We will further identify the subset of points that are consistent with the recently released 2018 Planck observation [36] of $\Omega h^2 = 0.120 \pm 0.001$. Regarding LHC gluino searches, a firm lower limit is imposed on the gluino mass of $M(\tilde{g}) \geq 1.6$ TeV, allowing for a reasonable lower boundary under all the LHC gluino searches.

The light Higgs boson mass theoretical calculation is allowed to float around the experimental central value of $m_h = 125.09$ GeV, though we do enforce a larger range of $123 \leq m_h \leq 128$ GeV to account for a 2σ experimental uncertainty over and above a theoretical uncertainty of 1.5 GeV in our computations. The actual numerical value of the flippon Yukawa coupling remains an unknown, hence we permit the Yukawa coupling to range from a minimum value to its maximum in our light Higgs boson mass computations. A minimal flippon Yukawa coupling does not allow any vector-like flippon contributions, as the light Higgs boson mass in this case is then comprised of only the 1-loop and 2-loop SUSY contributions, chiefly from the coupling to the light stop. A maximum flippon Yukawa coupling implies the (XD, XD^c)

flippon Yukawa coupling is fixed at $Y_{XD} = 0$ and the (XU, XU^c) flippon Yukawa coupling is set at $Y_{XU} = 1$, with the (XD, XD^c) flippon trilinear coupling A term set at $A_{XD} = 0$ and the (XU, XU^c) A term fixed at $A_{XU} = A_U = A_0$ [12, 13]. When necessary, we shall choose the maximum flippon Yukawa coupling in order to lift the light Higgs boson mass up to its observed value. However, some points in the model space can reach the Higgs boson observed value with no flippon contribution, thus we choose the minimal coupling in these instances. Regardless of our choice for the numerical value of the flippon Yukawa coupling, the calculation must return a value within $123 \leq m_h \leq 128$ GeV. For our chosen benchmarks points that are meant to be sufficiently representative of the model space, we will clearly annotate as to whether the given light Higgs boson mass consists of the minimum or maximum flippon Yukawa coupling.

The model space is additionally constrained via rare decay, direct dark matter detection, and proton decay experimental results. The rare decay experimental constraints include the branching ratio of the rare b-quark decay of $Br(b \rightarrow s\gamma) = (3.43 \pm 0.21^{stat} \pm 0.24^{th} \pm 0.07^{sys}) \times 10^{-4}$ [37], the branching ratio of the rare B-meson decay to a dimuon of $Br(B_s^0 \rightarrow \mu^+ \mu^-) = (2.9 \pm 0.7 \pm 0.29^{th}) \times 10^{-9}$ [38], and the 3σ intervals around the Standard Model result and experimental measurement of the SUSY contribution to the anomalous magnetic moment of the muon of $-17.7 \times 10^{-10} \leq \Delta a_\mu \leq 43.8 \times 10^{-10}$ [39]. Direct dark matter detection constraints encompass limits on spin-independent cross-sections for neutralino-nucleus interactions established by the Large Underground Xenon (LUX) experiment [40], PandaX-II Experiment [41], and XENON100 Collaboration [42], and limits on the proton spin-dependent cross-sections by the COUPP Collaboration [43] and XENON100 Collaboration [44]. Finally, we assess our $SU(5) \times U(1)_X$ grand unification against the current limits of about 1.7×10^{34} yrs on the proton decay rate $p \rightarrow e^+ \pi^0$ [45].

A total of 110 million points were randomly sampled in scans implementing the $SU(5) \times U(1)_X$ $M_{\mathcal{F}}$ scale boundary conditions, with only about 37,000 of those points surviving the applied constraints. The SUSY mass spectra, relic density, rare decay processes, and direct dark matter detection cross-sections are calculated with **MicrOMEGAs 2.1** [46] utilizing a proprietary mpi modification of the **SuSpect 2.34** [47] codebase to run flippon and General No-Scale \mathcal{F} - $SU(5)$ enhanced RGEs, employing non-universal soft supersymmetry breaking parameters at the $M_{\mathcal{F}}$ scale. Supersymmetric particle decays are computed with **SUSY-HIT 1.5a** [48]. The Particle Data Group [49] world average for the strong coupling constant is $\alpha_S(M_Z) = 0.1181 \pm 0.0011$ at 1σ , and we assume a value in this work of $\alpha_S = 0.1184$.

A total of 12 viable benchmark points are chosen to be reasonably representative of the model space for a given set of parameters $(M_5, M_{1X}, M_{U^c L}, M_{E^c}, M_{Q D^c N^c}, M_H,$

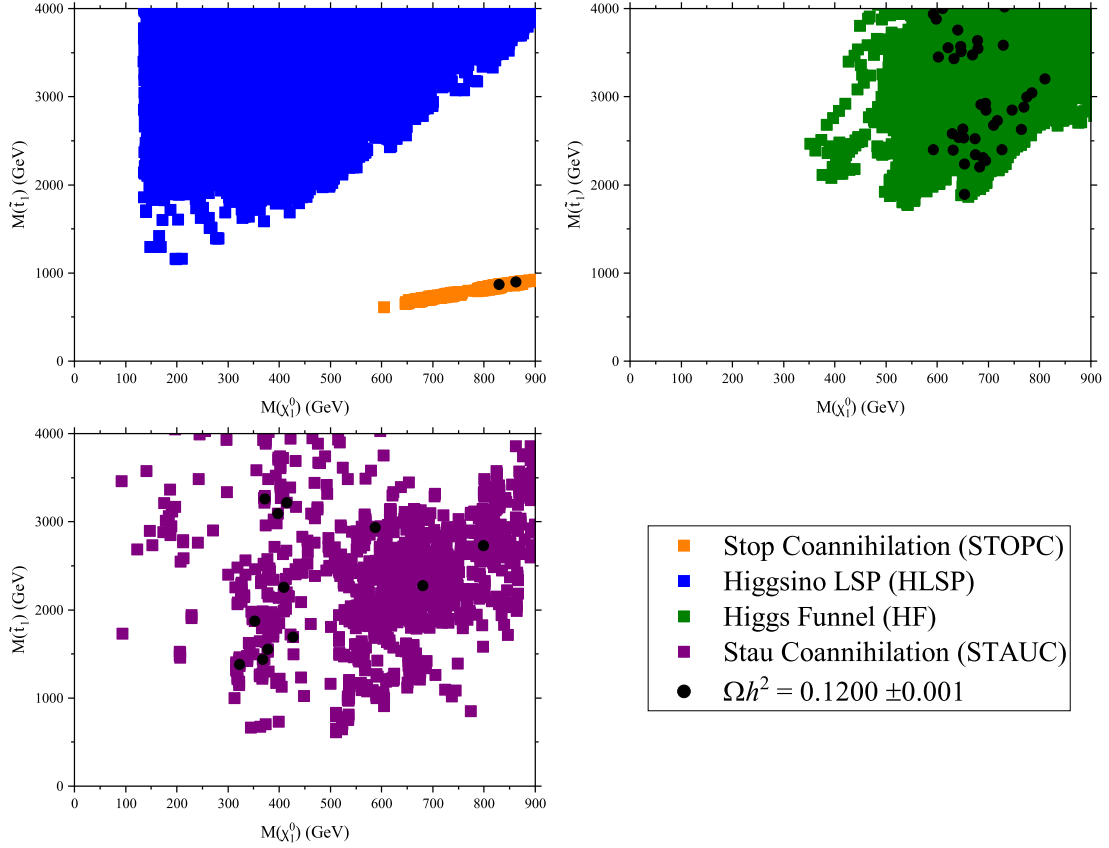


FIG. 1: Light stop mass $M(\tilde{t}_1)$ as a function of the lightest neutralino mass $M(\tilde{\chi}_1^0)$ for the four regions of the model space we study in this work. The stop coannihilation strip can be observed in the upper left plot space. Notice that there is no intersection between the Light Stop Coannihilation and pure Higgsino regions, though a more detailed analysis relaxing the higgsino and light stop coannihilation requirements we applied here is in progress [50] to ascertain any potential union of these two significant regions. All points plot satisfy the light Higgs boson mass and relic density observations we outlined in this work, in addition to rare decay and current LHC SUSY search constraints. The round black dots represent those points that can also satisfy the recent 2018 Planck Collaboration satellite relic density measurements of $\Omega h^2 = 0.120 \pm 0.001$.

$A_\tau, A_t, A_b, M_V, \tan\beta, M_t$). The data results are distributed across TABLES I - III. The benchmark models of TABLES I - III originate via categorization of the viable model space into four dissimilar regions identified by LSP and NLSP characteristics, to be discussed shortly. The numerical relic density figures annotated in TABLE III consist only of the SUSY lightest neutralino $\tilde{\chi}_1^0$ abundance, therefore regions with numerical values less than the WMAP9 1σ measurement lower bound of about $\Omega h^2 \simeq 0.1093$ must welcome alternative additions to the total observed relic density by WMAP9 and Planck. Given the potential for multi-component dark matter in regions of low neutralino density, the spin-dependent and spin-independent cross-section calculations provided in

TABLE III are rescaled per the following expression:

$$\sigma_{SI(SD)}^{\text{re-scaled}} = \sigma_{SI(SD)} \frac{\Omega h^2}{0.1138} \quad (17)$$

PHENOMENOLOGICAL RESULTS

The model space is constrained per the experimental constraints detailed in the prior section, with the exception of the LUX, PandaX-II, and XENON cross-sections, which we shall evaluate independently of all the other empirical measurements. Post application of the constraints, the surviving viable parameter space consists of four interesting regions segregated by LSP characteristics

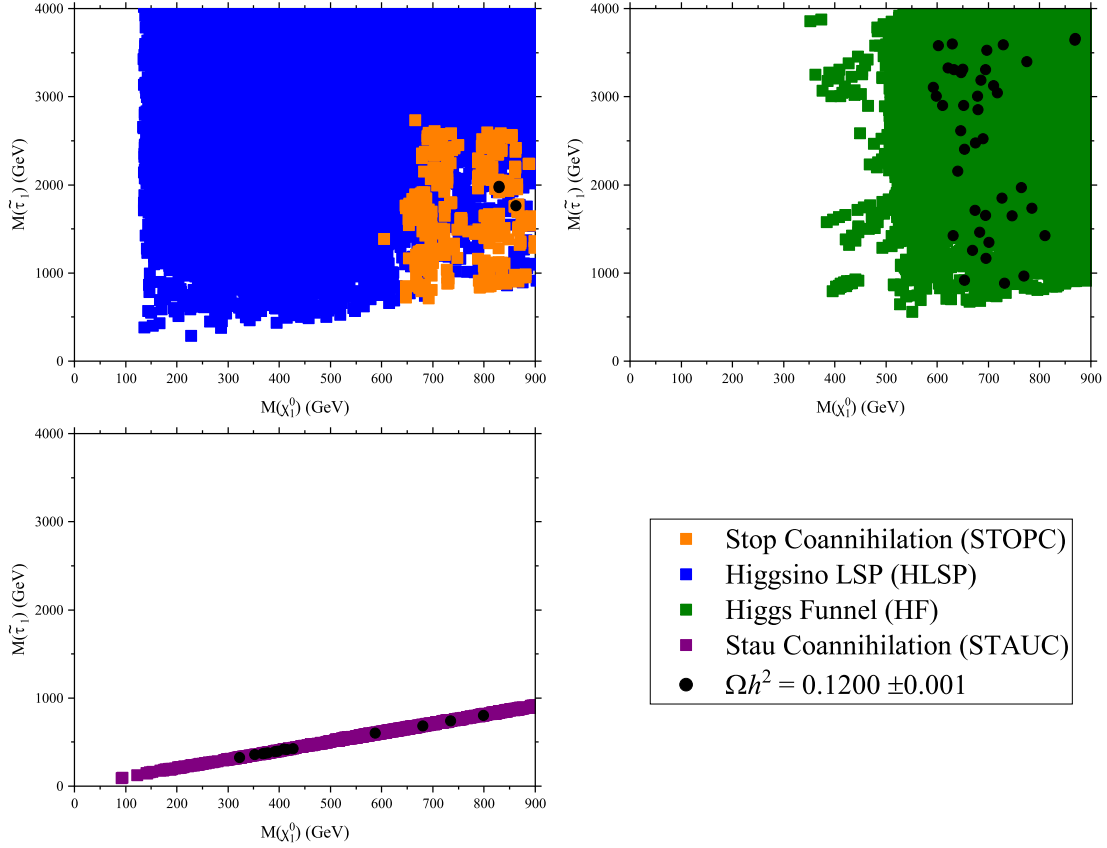


FIG. 2: Light tau mass $M(\tilde{\tau}_1)$ as a function of the lightest neutralino mass $M(\tilde{\chi}_1^0)$ for the four regions of the model space we study in this work. The tau coannihilation strip can be observed in the lower left plot space. All points plot satisfy the light Higgs boson mass and relic density observations we outlined in this work, in addition to rare decay and current LHC SUSY search constraints. The round black dots represent those points that can also satisfy the recent 2018 Planck Collaboration satellite relic density measurements of $\Omega h^2 = 0.120 \pm 0.001$.

and the NLSP. The four regions are identified as (i) light stop coannihilation (STOPC), with $M(\tilde{t}_1) - M(\tilde{\chi}_1^0) \leq 50$ GeV; (ii) pure higgsino LSP (HLSP), restricted to the conditions $M(\tilde{\chi}_2^0) - M(\tilde{\chi}_1^0) = 9 - 10$ GeV, $M(\tilde{\chi}_1^\pm) - M(\tilde{\chi}_1^0) = 3 - 7$ GeV, $M(\tilde{\chi}_2^0) < 0$, which consistently generates an LSP greater than 98% higgsino; (iii) Higgs Funnel (HF), with $M(H^0/A^0) \sim 2M(\tilde{\chi}_1^0)$, where we allow a tolerance of ± 100 GeV on $M(H^0/A^0)$; and (iv) light tau coannihilation (STAUC), with $M(\tilde{\tau}_1^\pm) - M(\tilde{\chi}_1^0) \leq 20$ GeV. The light stop coannihilation, Higgs Funnel, and light tau coannihilation regions all generate an LSP that is almost entirely bino. The lower mass boundaries of all these four regions are essentially defined by the LHC constraints, which include the gluino and other ATLAS and CMS search constraints we shall discuss in the forthcoming paragraphs.

The light stop (\tilde{t}_1) is the NLSP for all of the stop coannihilation points. The very narrow 2018 Planck relic density of $\Omega h^2 = 0.120 \pm 0.001$ can be generated with $M(\tilde{t}_1) - M(\tilde{\chi}_1^0) \simeq 35 - 40$ GeV. The STOPC region is illustrated in FIGs. 1 - 4, with FIG. 1 displaying the light stop mass as a function of the LSP $\tilde{\chi}_1^0$, clearly indicating the light stop coannihilation strip, with the lower end severed by the most recent LHC constraints. Given that the small mass delta we require is less than M_t , the light stop is forced into the decay channel $\tilde{t}_1 \rightarrow c + \tilde{\chi}_1^0$ and the gluino will always produce a light stop ($\tilde{g} \rightarrow \tilde{t}_1 t$), as highlighted in TABLE IV. The near degenerate LSP and light stop in this STOPC channel can evade the current ATLAS [51, 52] and CMS [53–56] LHC light stop searches. Applying the strongest constraints from both ATLAS and CMS on $M(\tilde{t}_1) - M(\tilde{\chi}_1^0)$ and $M(\tilde{t}_1)$ requires

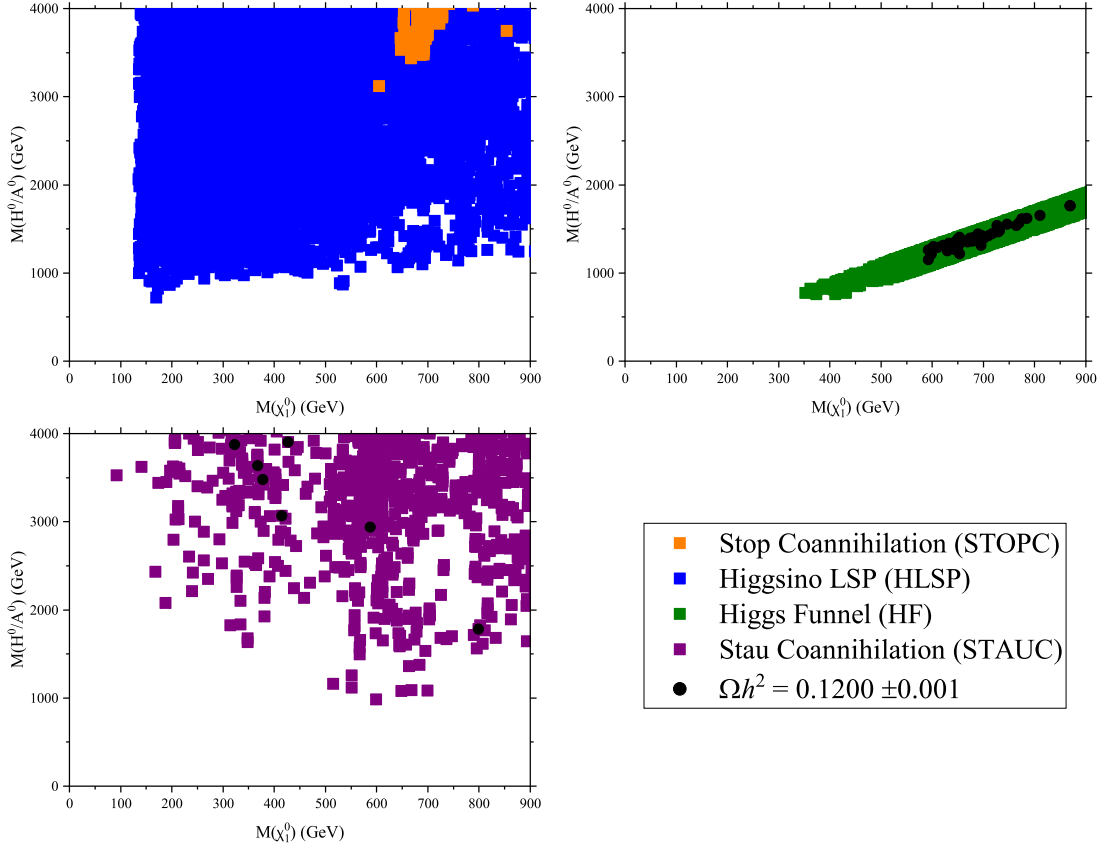


FIG. 3: Heavy neutral and pseudoscalar SUSY Higgs mass $M(H^0/A^0)$ as a function of the lightest neutralino mass $M(\tilde{\chi}_1^0)$ for the four regions of the model space we study in this work. The Higgs Funnel region can be observed in the upper right plot space. All points plot satisfy the light Higgs boson mass and relic density observations we outlined in this work, in addition to rare decay and current LHC SUSY search constraints. The round black dots represent those points that can also satisfy the recent 2018 Planck Collaboration satellite relic density measurements of $\Omega h^2 = 0.120 \pm 0.001$.

us to enforce $M(\tilde{t}_1) > 550$ GeV for our given mass delta of $M(\tilde{t}_1) - M(\tilde{\chi}_1^0) \leq 50$ GeV, defining the lower end of the light stop coannihilation strip in FIG. 1. This constraint is included in all of FIGs. 1 - 4.

The higgsino spectra are identified by the Higgs bilinear mass term μ driven via RGE running below the gaugino mass terms M_1 and M_2 at low-energy near electroweak symmetry breaking (EWSB), thus driving the $\tilde{\chi}_2^0$ mass negative. This is despite the fact that the μ term can be larger or smaller than the gaugino mass terms M_5 and M_{1X} at the $M_{\mathcal{F}}$ scale. The tight constraints applied within the higgsino region ensure an almost 100% higgsino LSP, though it apparently does prevent any combination of a pure higgsino LSP and light stop NLSP. This is evident in FIG. 1 by observing the gap between the HLSP and STOPC points, as no spectra with

$M(\tilde{t}_1) - M(\tilde{\chi}_1^0) \leq 50$ GeV can also generate a pure higgsino LSP. This notwithstanding, preliminary studies do show that a STOPC point with $M(\tilde{t}_1) - M(\tilde{\chi}_1^0) \leq 50$ GeV can possess an LSP that is dominantly higgsino, for example, more than 60% and potentially as high as 80% or greater. While we do not integrate this more detailed HLSP+STOPC analysis into this work, it is currently in progress [50]. Such a combination of a dominantly higgsino LSP and light stop NLSP is rather difficult to produce naturally [57], though it has been uncovered in certain realistic intersecting D6-brane models [58]. As a result of our tight constraints on the higgsino in order to generate a pure higgsino LSP, most of the higgsino points in FIGs. 1 - 4 have $M(\tilde{t}_1) > M(\tilde{g})$, thus we focus on these primary higgsino spectra here in this work. Unfortunately, as depicted in TABLE IV, there is

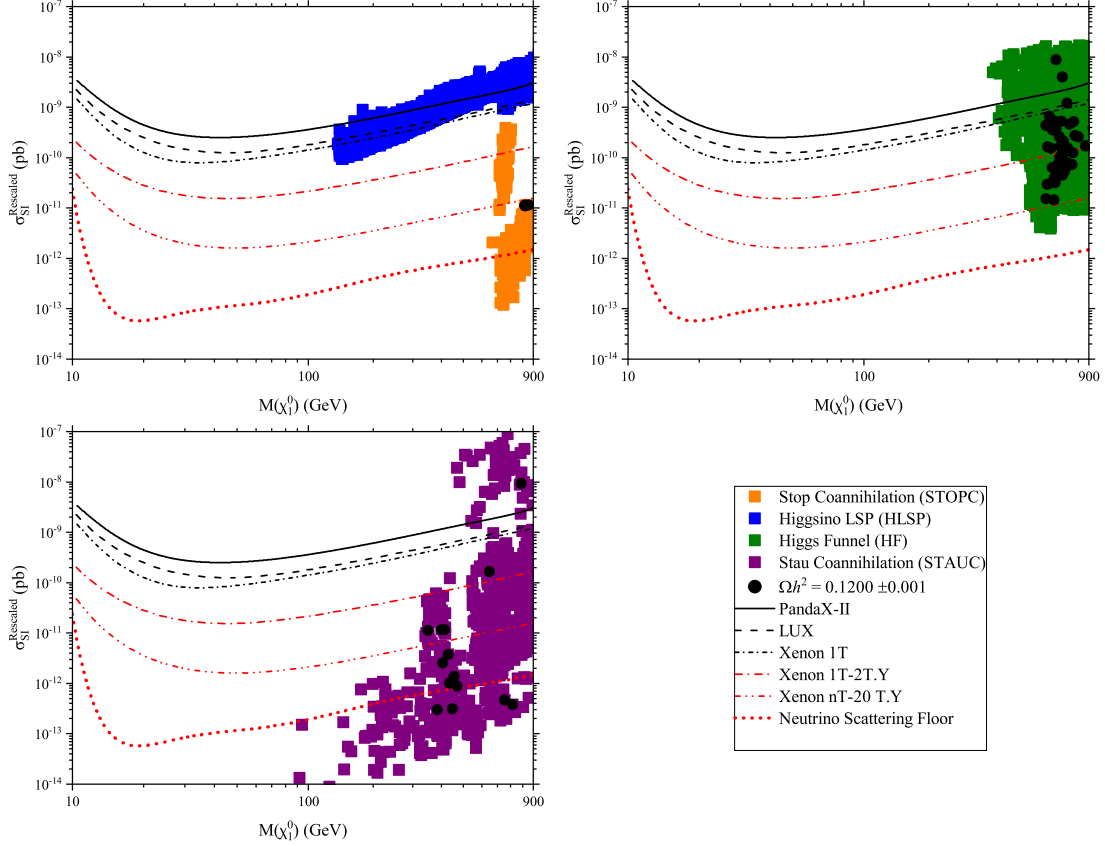


FIG. 4: Illustration of the PandaX-II, LUX, and XENON WIMP-nucleon spin-independent cross-section constraints applied to the model space studied in this work. The σ_{SI} cross-sections have been rescaled in accordance with Eq. (17). All points plot satisfy the light Higgs boson mass and relic density observations we outlined in this work, in addition to rare decay and current LHC SUSY search constraints. The round black dots represent those points that can also satisfy the recent 2018 Planck Collaboration satellite relic density measurements of $\Omega h^2 = 0.120 \pm 0.001$.

no dominant decay channel to consistent final states for either the light stop or gluino in the HLSP region. As can be inferred from TABLE IV and our constraint of $M(\tilde{\chi}_1^\pm) - M(\tilde{\chi}_1^0) = 3 - 7$ GeV, the chargino participates in the off-shell Standard Model boson mediated decays $\tilde{\chi}_1^\pm \rightarrow u\bar{d}/c\bar{s} + \tilde{\chi}_1^0$ (36%/36%) or $\tilde{\chi}_1^\pm \rightarrow l^\pm + \nu_l + \tilde{\chi}_1^0$ (28%), and these pure higgsino points have an LHC established lower bound of about $M(\tilde{\chi}_1^\pm) \sim 140$ GeV [59], thus we enforce $M(\tilde{\chi}_1^\pm) > 140$ GeV in FIGs. 1 - 4.

The chargino $\tilde{\chi}_1^\pm$ is the NLSP for 99.6% of the Higgs Funnel points, with the remaining 0.4% possessing a stau NLSP. Nonetheless, only 0.07% of the Higgs Funnel also resides in the $M(\tilde{\tau}_1^\pm) - M(\tilde{\chi}_1^0) \leq 20$ GeV stau coannihilation strip. We further observe that 11.5% of the Higgs Funnel has a dominant higgsino LSP, though only 0.5% are pure higgsino. The upper right plot space of FIG. 3

clearly shows the HF region with $M(H^0/A^0)$ plot as a function of the LSP $\tilde{\chi}_1^0$. The minimum heavy Higgs boson mass in the HF region is $M(H^0/A^0) \sim 800$ GeV, and these H^0/A^0 near this lower boundary all have $30 \leq \tan\beta \leq 40$, and given a branching ratio of more than 85% for $H^0/A^0 \rightarrow b\bar{b}$, the lightest $M(H^0/A^0)$ in our model space persist comfortably beyond current LHC constraints for BSM Higgs searches [60].

In our light stau coannihilation strip, only 27.6% of the points have stau NLSP, with the remaining 72.4% having a chargino $\tilde{\chi}_1^\pm$ NLSP. As one would expect though, four nearly degenerate sparticles ($\tilde{\chi}_1^0, \tilde{\chi}_1^\pm, \tilde{\chi}_2^0, \tilde{\tau}_1^\pm$) greatly suppresses the relic density, hence only the stau $\tilde{\tau}_1^\pm$ NLSP points with larger $\tilde{\chi}_1^\pm$ and $\tilde{\chi}_2^0$ in the light stau coannihilation strip can generate the observed WMAP9 and Planck relic density. The light stau coannihilation strip

TABLE IV: Dominant gluino (\tilde{g}) and light stop (\tilde{t}_1) decay modes for each of the regions of the model space we study in this work, along with the associated branching ratios. Here, $q = (u, d, c, s)$ and $\tilde{q} = (\tilde{u}, \tilde{d}, \tilde{c}, \tilde{s})$.

Model	Dominant Decay Mode	Branching Ratio
Stop Coannihilation	$\tilde{g} \rightarrow \tilde{t}_1 t$	100%
	$\tilde{t}_1 \rightarrow c + \tilde{\chi}_1^0$	80 – 98%
Pure Higgsino	$\tilde{g} \rightarrow \tilde{\chi}_1^\pm + t + b \rightarrow q\bar{q} + t + b + \tilde{\chi}_1^0$	$\sim 28\%$
	$\tilde{g} \rightarrow t\bar{t} + \tilde{\chi}_1^0$	$\sim 14\%$
	$\tilde{t}_1 \rightarrow \tilde{g} + t$	$\sim 32\%$
	$\tilde{t}_1 \rightarrow \tilde{\chi}_1^\pm + b \rightarrow q\bar{q} + b + \tilde{\chi}_1^0$	$\sim 16\%$
Higgs Funnel	$\tilde{g} \rightarrow \tilde{\chi}_1^\pm + t + b \rightarrow q\bar{q} + t + b + \tilde{\chi}_1^0$ [$M(\tilde{\chi}_1^\pm) - M(\tilde{\chi}_1^0) < M(W^\pm)$]	$\sim 21\%$
	$\tilde{g} \rightarrow \tilde{\chi}_1^\pm + t + b \rightarrow W^\pm + t + b + \tilde{\chi}_1^0$ [$M(\tilde{\chi}_1^\pm) - M(\tilde{\chi}_1^0) > M(W^\pm)$]	$\sim 26\%$
	<u>Larger $M(\tilde{t}_1) - M(\tilde{g})$</u>	
	$\tilde{t}_1 \rightarrow \tilde{g} + t$	$\sim 48\%$
	$\tilde{t}_1 \rightarrow \tilde{\chi}_1^\pm + b \rightarrow q\bar{q} + b + \tilde{\chi}_1^0$	$\sim 15\%$
	<u>Smaller $M(\tilde{t}_1) - M(\tilde{g})$</u>	
Stau Coannihilation	$\tilde{t}_1 \rightarrow \tilde{g} + t$	$\sim 18\%$
	$\tilde{t}_1 \rightarrow \tilde{\chi}_1^\pm + b \rightarrow W^\pm + b + \tilde{\chi}_1^0$	$\sim 39\%$
	<u>$M(\tilde{g}) - M(\tilde{t}_1) > M_t$</u>	
	$\tilde{g} \rightarrow \tilde{t}_1 t \rightarrow t\bar{t} + \tilde{\chi}_1^0$	$\sim 100\%$
	$\tilde{t}_1 \rightarrow t + \tilde{\chi}_1^0$	$\sim 100\%$
	<u>$M(\tilde{g}) - M(\tilde{t}_1) < M_t$</u>	
	$\tilde{g} \rightarrow t\bar{t} + \tilde{\chi}_1^0$	$\sim 6\%$
	$\tilde{t}_1 \rightarrow \tilde{\chi}_1^\pm + b \rightarrow \tilde{\tau}_1^\pm + \nu_\tau + b \rightarrow \tau^\pm + \nu_\tau + b + \tilde{\chi}_1^0$	$\sim 18\%$

is evident in the lower left panel of FIG. 2. We inspect the most recent ATLAS slepton constraints [59] on compressed spectra, such as we have in the STAUC region, therefore we attempt to approximately emulate the ATLAS slepton exclusions by applying the following constraints on our model space, where both conditions for each must be TRUE for the point to be excluded: (1) $M(\tilde{\tau}_1^\pm) < 100$ GeV and $M(\tilde{\tau}_1^\pm) - M(\tilde{\chi}_1^0) > 1$ GeV; (2) $100 \leq M(\tilde{\tau}_1^\pm) < 150$ GeV and $2 \leq M(\tilde{\tau}_1^\pm) - M(\tilde{\chi}_1^0) \leq 14$ GeV; and (3) $150 \leq M(\tilde{\tau}_1^\pm) < 190$ GeV and $3 \leq M(\tilde{\tau}_1^\pm) - M(\tilde{\chi}_1^0) \leq 8$ GeV. These restrictions are included in FIGs. 1 - 4. Notice in constraint (1) just above that we allow for an off-shell tau lepton τ^\pm less than 1 GeV, an

action that does capture a not insignificant number of viable points, in view of the fact that 10.5% of the STAUC region has $M(\tilde{\tau}_1^\pm) - M(\tilde{\chi}_1^0) < 1$ GeV. A quick review of TABLE IV indicates that the stau coannihilation spectra with light stau NLSP and $M(\tilde{g}) - M(\tilde{t}_1) > M_t$ produce exclusively a 4-top signature ($\tilde{g} \rightarrow \tilde{t}_1 t \rightarrow t\bar{t} + \tilde{\chi}_1^0$), giving rise to large multijet events, as is typical in $\mathcal{F}\text{-}SU(5)$ [20]. The final states are not as clear when $M(\tilde{g}) - M(\tilde{t}_1) < M_t$ or $M(\tilde{g}) < M(\tilde{t}_1)$ given that there is no dominant decay channel in either of these two cases. The model space is generally split between these two situations, where about half the STAUC region has $M(\tilde{g}) - M(\tilde{t}_1) > M_t$ and the other half of the STAUC region has $M(\tilde{g}) - M(\tilde{t}_1) < M_t$

or $M(\tilde{g}) < M(\tilde{t}_1)$.

CONCLUSION

With our motivation partially inspired by D-brane model building, we presented an analysis of non-zero general SUSY breaking soft terms in \mathcal{F} - $SU(5)$. The methodology involved massive parallel computing given the large number of unknown parameters. While the resulting viable parameter space was extraordinarily constrained given the large number of computations, several interesting regions were uncovered that can simultaneously generate the WMAP and Planck observed relic density measurements and correct light Higgs boson mass, over and above satisfying many LHC search constraints. Four regions that accomplish these rely upon (i) light stop coannihilation, (ii) pure Higgsino dark matter, (iii) Higgs funnel, and (iv) light stau coannihilation, though the pure Higgsino LSP could not reach the observed relic density due to its large annihilation cross-section. Concluding the analysis was an effort to identify the decay modes to final states that could represent observable signatures of these four scenarios, discovering that the light stop coannihilation and light stau coannihilation decay channels possess very dominant branching fractions. The light stop coannihilation produces the typical top+charm quark final state via the gluino decay and the light stau coannihilation mostly leads to the characteristic \mathcal{F} - $SU(5)$ large multijet event, whereas the pure Higgsino LSP and Higgs funnel provide no dominant decay channel to final states. Though possibly furnishing the highest intrigue, our exploration tentatively revealed that the \mathcal{F} - $SU(5)$ model may indeed harbor a rather diminutive region exhibiting spectra with a mixed scenario of a dominant Higgsino LSP *and* light stop coannihilation, a rare yet rather natural SUSY spectrum, but that is the focus of our next endeavor.

ACKNOWLEDGMENTS

Portions of this research were conducted with high performance computational resources provided by the Louisiana Optical Network Infrastructure (<http://www.loni.org>). This research was supported in part by the Projects 11475238, 11647601, and 11875062 supported by the National Natural Science Foundation of China (TL), and by the DOE grant DE-FG02-13ER42020 (DVN).

the ATLAS detector at the LHC,” Phys. Lett. **B716**, 1 (2012), 1207.7214.

- [2] S. Chatrchyan et al. (CMS), “Observation of a new boson at a mass of 125 GeV with the CMS experiment at the LHC,” Phys. Lett. **B716**, 30 (2012), 1207.7235.
- [3] M. Carena, S. Gori, N. R. Shah, and C. E. M. Wagner, “A 125 GeV SM-like Higgs in the MSSM and the $\gamma\gamma$ rate,” JHEP **03**, 014 (2012), 1112.3336.
- [4] W. Adam, “Searches for SUSY, talk at the 38th International Conference on High Energy Physics,” (2016).
- [5] S. M. Barr, “A New Symmetry Breaking Pattern for $SO(10)$ and Proton Decay,” Phys. Lett. **B112**, 219 (1982).
- [6] J. P. Derendinger, J. E. Kim, and D. V. Nanopoulos, “Anti- $SU(5)$,” Phys. Lett. **B139**, 170 (1984).
- [7] I. Antoniadis, J. R. Ellis, J. S. Hagelin, and D. V. Nanopoulos, “Supersymmetric Flipped $SU(5)$ Revitalized,” Phys. Lett. **B194**, 231 (1987).
- [8] J. Jiang, T. Li, and D. V. Nanopoulos, “Testable Flipped $SU(5) \times U(1)_X$ Models,” Nucl. Phys. **B772**, 49 (2007), hep-ph/0610054.
- [9] J. Jiang, T. Li, D. V. Nanopoulos, and D. Xie, “F- $SU(5)$,” Phys. Lett. **B677**, 322 (2009), 0811.2807.
- [10] J. Jiang, T. Li, D. V. Nanopoulos, and D. Xie, “Flipped $SU(5) \times U(1)_X$ Models from F-Theory,” Nucl. Phys. **B830**, 195 (2010), 0905.3394.
- [11] J. L. Lopez, D. V. Nanopoulos, and K.-j. Yuan, “The Search for a realistic flipped $SU(5)$ string model,” Nucl. Phys. **B399**, 654 (1993), hep-th/9203025.
- [12] T. Li, J. A. Maxin, D. V. Nanopoulos, and J. W. Walker, “A Higgs Mass Shift to 125 GeV and A Multi-Jet Supersymmetry Signal: Miracle of the Flippons at the $\sqrt{s} = 7$ TeV LHC,” Phys.Lett. **B710**, 207 (2012), 1112.3024.
- [13] Y. Huo, T. Li, D. V. Nanopoulos, and C. Tong, “The Lightest CP-Even Higgs Boson Mass in the Testable Flipped $SU(5) \times U(1)_X$ Models from F-Theory,” Phys.Rev. **D85**, 116002 (2012), 1109.2329.
- [14] T. Li, D. V. Nanopoulos, and J. W. Walker, “Fast Proton Decay,” Phys. Lett. **B693**, 580 (2010), 0910.0860.
- [15] T. Li, D. V. Nanopoulos, and J. W. Walker, “Elements of F-fast Proton Decay,” Nucl. Phys. **B846**, 43 (2011), 1003.2570.
- [16] E. Cremmer, S. Ferrara, C. Kounnas, and D. V. Nanopoulos, “Naturally Vanishing Cosmological Constant in $N = 1$ Supergravity,” Phys. Lett. **B133**, 61 (1983).
- [17] T. Li, J. A. Maxin, D. V. Nanopoulos, and J. W. Walker, “The Golden Point of No-Scale and No-Parameter \mathcal{F} - $SU(5)$,” Phys. Rev. **D83**, 056015 (2011), 1007.5100.
- [18] T. Li, J. A. Maxin, D. V. Nanopoulos, and J. W. Walker, “The Golden Strip of Correlated Top Quark, Gaugino, and Vectorlike Mass In No-Scale, No-Parameter \mathcal{F} - $SU(5)$,” Phys. Lett. **B699**, 164 (2011), 1009.2981.
- [19] T. Li, J. A. Maxin, D. V. Nanopoulos, and J. W. Walker, “The Unification of Dynamical Determination and Bare Minimal Phenomenological Constraints in No-Scale \mathcal{F} - $SU(5)$,” Phys.Rev. **D85**, 056007 (2012), 1105.3988.
- [20] T. Li, J. A. Maxin, D. V. Nanopoulos, and J. W. Walker, “The Ultrahigh jet multiplicity signal of stringy no-scale \mathcal{F} - $SU(5)$ at the $\sqrt{s} = 7$ TeV LHC,” Phys.Rev. **D84**, 076003 (2011), 1103.4160.
- [21] G. Giudice and A. Masiero, “A Natural Solution to the mu Problem in Supergravity Theories,” Phys. Lett. **B206**, 480 (1988).

[1] G. Aad et al. (ATLAS), “Observation of a new particle in the search for the Standard Model Higgs boson with

- [22] T. Leggett, T. Li, J. A. Maxin, D. V. Nanopoulos, and J. W. Walker, “No Naturalness or Fine-tuning Problems from No-Scale Supergravity,” (2014), 1403.3099.
- [23] T. Leggett, T. Li, J. A. Maxin, D. V. Nanopoulos, and J. W. Walker, “Confronting Electroweak Fine-tuning with No-Scale Supergravity,” *Phys.Lett.* **B740**, 66 (2015), 1408.4459.
- [24] T. Li, J. A. Maxin, and D. V. Nanopoulos, “The return of the King: No-Scale \mathcal{F} -SU(5),” *Phys. Lett.* **B764**, 167 (2017), 1609.06294.
- [25] T. Li, J. A. Maxin, and D. V. Nanopoulos, “Probing the No-Scale \mathcal{F} -SU(5) one-parameter model via gluino searches at the LHC2,” *Phys. Lett.* **B773**, 54 (2017), 1705.07973.
- [26] C.-M. Chen, T. Li, and D. V. Nanopoulos, “Flipped and unflipped SU(5) as type IIA flux vacua,” *Nucl. Phys.* **B751**, 260 (2006), hep-th/0604107.
- [27] T. Li, J. A. Maxin, D. V. Nanopoulos, and J. W. Walker, “No-Scale \mathcal{F} -SU(5) in the Light of LHC, Planck and XENON,” *Jour.Phys.* **G40**, 115002 (2013), 1305.1846.
- [28] ATLAS, “Exotics Combined Summary Plots,” (2016), atlas.web.cern.ch/Atlas/GROUPS/PHYSICS/Combined-SummaryPlots/EXOTICS/index.html.
- [29] R. Harnik, D. T. Larson, H. Murayama, and M. Thormeier, “Probing the Planck scale with proton decay,” *Nucl.Phys.* **B706**, 372 (2005), hep-ph/0404260.
- [30] J. R. Ellis, D. V. Nanopoulos, and K. A. Olive, “Flipped heavy neutrinos: From the solar neutrino problem to baryogenesis,” *Phys.Lett.* **B300**, 121 (1993), hep-ph/9211325.
- [31] J. R. Ellis, J. L. Lopez, D. V. Nanopoulos, and K. A. Olive, “Flipped angles and phases: A Systematic study,” *Phys.Lett.* **B308**, 70 (1993), hep-ph/9303307.
- [32] T. Li, J. A. Maxin, D. V. Nanopoulos, and J. W. Walker, “Dark Matter, Proton Decay and Other Phenomenological Constraints in \mathcal{F} -SU(5),” *Nucl. Phys.* **B848**, 314 (2011), 1003.4186.
- [33] T. A. Aaltonen (Tevatron Electroweak Working Group, CDF, D0), “Combination of CDF and D0 results on the mass of the top quark using up to 8.7 fb^{-1} at the Tevatron,” (2013), 1305.3929.
- [34] G. Hinshaw et al. (WMAP), “Nine-Year Wilkinson Microwave Anisotropy Probe (WMAP) Observations: Cosmological Parameter Results,” *Astrophys. J. Suppl.* **208**, 19 (2013), 1212.5226.
- [35] P. A. R. Ade et al. (Planck), “Planck 2015 results. XIII. Cosmological parameters,” *Astron. Astrophys.* **594**, A13 (2016), 1502.01589.
- [36] N. Aghanim et al. (Planck), “Planck 2018 results. VI. Cosmological parameters,” (2018), 1807.06209.
- [37] HFAG (2013), www.slac.stanford.edu/xorg/hfag/rare/2013/radll/OUTPUT/TABLES/radll.pdf.
- [38] V. Khachatryan et al. (LHCb, CMS), “Observation of the rare $B_s^0 \rightarrow \mu^+ \mu^-$ decay from the combined analysis of CMS and LHCb data,” *Nature* **522**, 68 (2015), 1411.4413.
- [39] T. Aoyama, M. Hayakawa, T. Kinoshita, and M. Nio, “Complete Tenth-Order QED Contribution to the Muon $g-2$,” *Phys.Rev.Lett.* **109**, 111808 (2012), 1205.5370.
- [40] D. S. Akerib et al., “Results from a search for dark matter in LUX with 332 live days of exposure,” (2016), 1608.07648.
- [41] A. Tan et al. (PandaX-II), “Dark Matter Results from First 98.7-day Data of PandaX-II Experiment,” *Phys. Rev. Lett.* **117**, 121303 (2016), 1607.07400.
- [42] E. Aprile et al. (XENON), “Dark Matter Search Results from a One Tonne \times Year Exposure of XENON1T,” (2018), 1805.12562.
- [43] E. Behnke et al. (COUPP), “First Dark Matter Search Results from a 4-kg CF₃I Bubble Chamber Operated in a Deep Underground Site,” *Phys. Rev.* **D86**, 052001 (2012), [Erratum: *Phys. Rev.D*90,no.7,079902(2014)], 1204.3094.
- [44] E. Aprile et al. (XENON100), “Limits on spin-dependent WIMP-nucleon cross sections from 225 live days of XENON100 data,” *Phys. Rev. Lett.* **111**, 021301 (2013), 1301.6620.
- [45] V. Takhistov (Super-Kamiokande), in *Proceedings, 51st Rencontres de Moriond on Electroweak Interactions and Unified Theories: La Thuile, Italy, March 12-19, 2016* (2016), pp. 437–444, 1605.03235.
- [46] G. Belanger, F. Boudjema, A. Pukhov, and A. Semenov, “Dark matter direct detection rate in a generic model with micrOMEGAs2.1,” *Comput. Phys. Commun.* **180**, 747 (2009), 0803.2360.
- [47] A. Djouadi, J.-L. Kneur, and G. Moultaka, “SuSpect: A Fortran code for the supersymmetric and Higgs particle spectrum in the MSSM,” *Comput. Phys. Commun.* **176**, 426 (2007), hep-ph/0211331.
- [48] A. Djouadi, M. M. Muhlleitner, and M. Spira, “Decays of supersymmetric particles: The Program SUSY-HIT (SuSpect-SdecaY-Hdecay-InTerface),” *Acta Phys. Polon.* **B38**, 635 (2007), hep-ph/0609292.
- [49] C. Patrignani et al. (Particle Data Group), “Review of Particle Physics,” *Chin. Phys.* **C40**, 100001 (2016).
- [50] R. De Benedetti, T. Li, J. A. Maxin, and D. V. Nanopoulos (2018), in Preparation.
- [51] M. Aaboud et al. (ATLAS), “Search for dark matter and other new phenomena in events with an energetic jet and large missing transverse momentum using the ATLAS detector,” *JHEP* **01**, 126 (2018), 1711.03301.
- [52] M. Aaboud et al. (ATLAS), “Search for supersymmetry in final states with charm jets and missing transverse momentum in 13 TeV pp collisions with the ATLAS detector,” (2018), 1805.01649.
- [53] A. M. Sirunyan et al. (CMS), “Search for the pair production of third-generation squarks with two-body decays to a bottom or charm quark and a neutralino in proton-proton collisions at $\sqrt{s} = 13\text{ TeV}$,” *Phys. Lett.* **B778**, 263 (2018), 1707.07274.
- [54] A. M. Sirunyan et al. (CMS), “Search for new phenomena with the M_{T2} variable in the all-hadronic final state produced in proton-proton collisions at $\sqrt{s} = 13\text{ TeV}$,” *Eur. Phys. J.* **C77**, 710 (2017), 1705.04650.
- [55] A. M. Sirunyan et al. (CMS), “Search for direct production of supersymmetric partners of the top quark in the all-jets final state in proton-proton collisions at $\sqrt{s} = 13\text{ TeV}$,” *JHEP* **10**, 005 (2017), 1707.03316.
- [56] A. M. Sirunyan et al. (CMS), “Search for natural and split supersymmetry in proton-proton collisions at $\sqrt{s} = 13\text{ TeV}$ in final states with jets and missing transverse momentum,” *JHEP* **05**, 025 (2018), 1802.02110.
- [57] J. Ellis, J. L. Evans, F. Luo, K. A. Olive, and J. Zheng, “Stop Coannihilation in the CMSSM and SubGUT Models,” *Eur. Phys. J.* **C78**, 425 (2018), 1801.09855.
- [58] W. Ahmed, L. Calibbi, T. Li, S. Raza, J.-S. Niu, and X.-C. Wang, “Naturalness and Dark Matter in a Realistic Intersecting D6-Brane Model,” *JHEP* **06**, 126 (2018),

- 1711.10225.
- [59] M. Aaboud et al. (ATLAS), “Search for electroweak production of supersymmetric states in scenarios with compressed mass spectra at $\sqrt{s} = 13$ TeV with the ATLAS detector,” Phys. Rev. **D97**, 052010 (2018), 1712.08119.
- [60] A. M. Sirunyan et al. (CMS), “Search for beyond the standard model Higgs bosons decaying into a $b\bar{b}$ pair in pp collisions at $\sqrt{s} = 13$ TeV,” (2018), 1805.12191.